Spatial Vision, Vol. 11, No. 3, pp. 295–313 (1998)

Spatio-temporal vernier acuity

ANDREI GOREA* and STEPHEN T. HAMMETT†

Laboratoire de Psychologie Expérimentale, René Descartes University and C.N.R.S., 28 rue Serpente, 75006 Paris, France

Received 13 October 1997; revised 15 December 1997; accepted 17 December 1997

Abstract—The study of space-time vernier (STV) provides information on the spatio-temporal structure of the visual system in the same way that the classical spatio-spatial vernier (SSV) provides information on its spatial structure. The transposition of a SSV task into a STV one yields the following experimental format: an object (in the present case a Gaussian blob) drifts with a constant velocity, V, disappears at x_0, t_0 and reappears after a variable duration Δt at a position $x_1 \pm \delta x$ with x_1 the correct position (given a constant V) and δx the minimum (positive and negative) spatial offset discriminable from x_0, i.e. the STV threshold. Observer's task is to specify whether the reappearance position is ahead of, or behind x_1.

The STV functions of Δt measured for 1, 5 and 10 deg/s reference velocities are linear with non-zero spatial and temporal intercepts at the origin. We refer to these x and t intercepts as *dynamic* $d_{\min}$ and $t_{\min}$. Dynamic $d_{\min}$ is the smallest instantaneous displacement (infinite velocity) discriminable from a continuous drift, V. Dynamic $t_{\min}$ is the shortest 'motion stop' discriminable from the same continuous drift, V. To our knowledge these quantities have not yet been assessed. Estimated dynamic $d_{\min}$ increases with V, whereas $t_{\min}$ is more or less V independent suggesting that the motion sensors presumably involved in the STV task have peak spatial frequencies inversely proportional with V and a temporal frequency characteristic independent of V (at least within the studied range).

The observed STV linearity with the spatio-temporal separation implies that the STV task is equivalent to a velocity discrimination. Two additional observations yield support to this conclusion. (i) The slopes of these functions yield velocities very similar to those discriminable from the reference V in a standard V-discrimination experiment. (ii) The predicted STV performances based on a decomposition of the task into two velocity discrimination tasks run as independent experiments are reasonably accurate.

INTRODUCTION

Vernier acuity has been defined as a purely spatial task. As noted by Adelson and Bergen (1991), a complete representation of the visual world (the *plenoptic function*) involves, however, psychophysical tasks which are of the vernier-acuity type but in space-time. To our knowledge, spatio-temporal vernier (STV) has not yet been measured.

*To whom correspondence should be addressed. E-mail: gorea@ext.jussieu.fr

†Present address: Department of Psychology, University of Glasgow, 62 Hillhead Str., Glasgow G12 8QQ, UK.

By analogy with the classical, spatio-spatial vernier (SSV), STV performances may be looked upon in a number of different ways. The standard view is that performances of this type (SSV, resolution, bisection, separation discrimination, curvature, etc.) can be accounted for in terms of the spatial frequency and orientation characteristics of the underlying receptive fields (Wilson, 1985, 1986; see reviews by McKee, 1991; Morgan, 1991). As such, it involves a number of free parameters (or assumptions) constraining the subserving mechanisms (as to their shape, bandwidth, sensitivity, overlap, etc.) and, as a consequence, does not yield 'intuitive' predictions of the measured performances. The standard view has been challenged by 'local-sign' models originally advocated by Hering (1889) and more recently developed by Watt and Morgan (1983), Morgan *et al.* (1990), Burbeck (1987, 1988), Burbeck and Yap (1990). Insofar as this local-position approach essentially applies for large separations, presumably not covered by one single receptive field, it is not directly relevant to the present STV study. As it is discussed below, the interpretation of our data is constrained by the assumption that the spatio-temporal separations used here are *within* the integration area of a motion sensitive receptive field.

Alternatives to the standard view essentially consist in relating SSV tasks to (or 'translating' them into) other, well documented tasks. SSV performances have been related to both *orientation* (Andrews *et al.*, 1973; Watt *et al.*, 1983) and *contrast discrimination* (e.g. Morgan and Aiba, 1985). Klein and col. (Klein *et al.*, 1990; Hu *et al.*, 1993; Carney and Klein, 1997) noted that most of the stimuli used in SSV tasks can be decomposed into a pedestal (the reference) and a pedestal plus an n-pole contrast modulation. Accordingly, position discrimination can be looked upon as (and expressed in terms of) a contrast discrimination task. Whilst both these approaches should be, in principle, derivable (though not in a trivial way) from the standard view, their main advantage is to circumvent a full-fledged characterization of the underlying mechanisms. They can be regarded as empirical shortcuts of the standard approach (see Carney and Klein, 1997). Moreover, they allow for intuitive predictions of the outcome of SSV tasks based on the empirical data collected in orientation and/or contrast discrimination experiments. The case in point within the context of the present experiments is the dependence of vernier acuity on the separation between the two vernier lines. The standard approach yields no intuition as to the expected outcome (which will depend heavily on both the parameters chosen and the implemented decision rules). Instead, the view that vernier acuity is but a variant of orientation discrimination yields the straightforward prediction that, beyond some critical separation, the vernier threshold should be proportional to the separation of the reference features, that is, it should respect Weber's law. This prediction has been confirmed by a number of studies (see Burbeck, 1987, 1988; Levi *et al.*, 1988; Levi and Klein, 1990). Weber's law for separation does not necessarily follow from either the standard model, or the contrast discrimination approach.

Insofar as SSV performances can be accounted for in terms of orientation discriminability in space-space, it is natural to assume that STV performances might reflect the *space–time orientation* discriminability, that is, velocity discrimination (Adelson and Bergen, 1985, 1991). This is to say that STV thresholds as a function of the

spatio-temporal gap should lie along a straight line (i.e. constant velocity) in space-time. As for the SSV case, this needs not be the prediction of alternative theoretical approaches. For example, the STV task could be envisaged as an *acceleration* detection task. Whilst this may not be a reasonable assumption,[1] many other alternatives do exist. Line element models (Wilson and Gelb, 1984; Wilson, 1986) will pose that a spatio-temporal offset is coded as the difference in the pooled responses of the subserving motion sensors and, as such, will bear predictions not related (or at least not *directly* related) to velocity discrimination. Failure of these models to predict vernier thresholds over a large separation range[2] led some authors to introduce the notion of *different visual strategies* or *cues* used in such tasks. For example, Klein and Levi (1987) suggested that vernier thresholds can reflect some sort of cortical measurement process limited by the positional uncertainty of the retinocortical mapping. Although such a strategy may (but does not need to) yield a Weber's law regime (for large separations), it is definitely not related to the system's capability of discriminating orientation in space–space or in space–time. Thus, Weber's law behavior for separation is not a proof that vernier thresholds directly reflect orientation discrimination. Such a proof would also require that the observed Weber's ratio directly translates into the observed orientation discrimination threshold measured under similar conditions.[3] This is the strategy adopted in the present study. The main question it has been designed to ask is whether or not STV performances reduce to velocity discrimination ones. This has been examined over a range of spatio-temporal separations and speeds by means of three independent experiments.

ANALYSIS AND DECOMPOSITION OF THE STV TASK

Analysis

Figure 1 displays space–time (x–t) diagrams of an object moving at a constant velocity, $V = \mathrm{ctg}(\alpha)$, disappearing at x_0, t_0 and reappearing Δt seconds later at some position $x_1 \pm \delta x$, with x_1, the position where it should have reappeared on the assumption of a constant V and with δx, the quantity to be experimentally varied so that it be just discriminable from x_1 (Fig. 1a).

The functions relating $\pm\delta x$ and Δt (or, for that matter, $\pm\delta t$ and Δx) are yet to be established and they are arbitrarily shown in Fig. 1b as hyperbolic. Their intersection with the space and time axes are referred to as *dynamic* $d_{\min}$ and $t_{\min}$, respectively (see Fig. 1b). These quantities measure the minimum visible *instantaneous* spatial displacement (i.e. at infinite V) and the minimum visible temporal gap at the *same spatial location* (i.e. zero V or 'motion stop').

Whilst for SSV tasks, both the theory and the data point to the symmetry of the incremental and decremental thresholds with respect to the reference orientation (dashed oblique line in Fig. 1), there is no reason to assume that this symmetry will hold in space-time.[4] Given the incommensurability of space and time, there is no a priori way to compare the spatial ($d_{\min}$) and temporal ($t_{\min}$) intercepts at the origin (for $\Delta t = 0$ and for $\Delta x = 0$, respectively), nor to attach a meaning to the x, t slopes

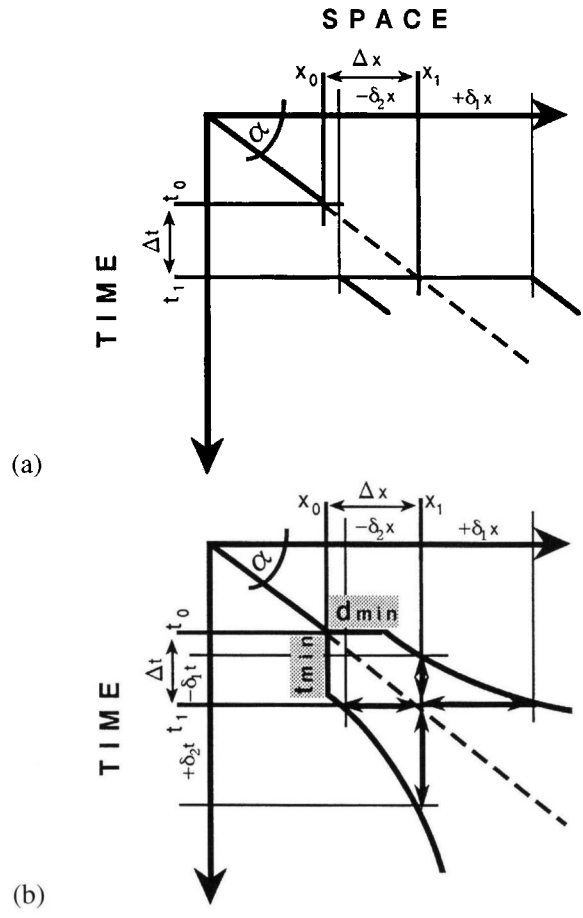

Figure 1. Space–time (x–t) diagrams of an object moving at a constant velocity, ctg(α), disappearing at x_0, t_0 and reappearing Δt seconds later at some position $x_1 \pm \delta x$, with δx the quantity to be experimentally varied so that it be liminarly visible. In (b), the $\pm\delta x$ vs Δt functions are arbitrarily shown as hyperbolic. $d_{\min}$ and $t_{\min}$ represent the intercepts of these functions at t_0 and x_0, respectively. The double-arrow lines in (b) show that $-\delta t$ thresholds can be inferred from $+\delta x$ ones (and reciprocally) but that there is no a priori constraint allowing the inference of negative offsets from positive ones along the same dimension (i.e. x or t).

of the two threshold functions. On these grounds the decremental thresholds cannot be derived from the incremental ones and both must be measured independently. It is worth noting that for linear STV threshold functions with a non-zero intercept at the origin, the assessment of the $\pm\delta x$ thresholds for two Δt (i.e. four experimental points) determines the whole STV space (for a given V). One of the purposes of the present study was to test this linearity; $\pm\delta x$ thresholds were measured for five Δt.

Since for each reference point x_1, t_1, a *positive* (and *negative*) *spatial* offset, $+\delta_1 x$, is equivalent to a *negative* (and *positive*) *temporal* offset, $-\delta_2 t$, STV functions can be assessed by measuring either of the two. Trivial as it is, this observation has not been taken advantage of in the literature probably because previous experimental designs

did not allow discrimination between positive and negative spatial (or temporal) offsets (e.g. Burr, 1979; Fahle and Poggio, 1981). Inferring δt thresholds from δx ones is economical and advantageous in visual psychophysics since current video equipment is typically much more limited in temporal (60 or 120 Hz) than in spatial (1024 pixels) resolution.

Decomposition

For the STV task to be feasible, the observer must:

- estimate the velocity of the *continuous motion* (CM) before the disappearance of the stimulus with an accuracy s_{CM};
- infer/estimate the velocity yielded by the space time coordinates of the disappearance (x_0, t_0 in Fig. 1) and reappearance (x_i, t_j) events; this task will be referred to as the *2-Flash* (2F) condition; the standard deviation of this estimate is s_{2F};
- compare the two estimates in the STV task with an accuracy $s_{STV} = ((s_{CM}^2 + s_{2F}^2)/2)^{1/2}$ (Macmillan and Creelman, 1991).[5]

According to this 'decomposition', STV performances should be predictable from independent assessments of CM and 2F velocity discrimination performances (see Appendix). These two additional tasks were thus performed as well.

To avoid confounding the spatio-temporal gap effect on the STV thresholds with eccentricity related effects (see Levi *et al.*, 1988; Levi and Klein, 1990), the stimuli in all experiments were displayed on a circular path centered around the fovea. Rotary motion has been shown to be mediated by local estimations of linear velocity (Werkhoven and Koenderink, 1991) and thus the present results may be generalized to the case of linear motion.

METHODS

The three experiments are illustrated in Fig. 2. Stimuli were displayed on a 19″ Sony video screen (1280 × 1024 pixels) under the control of a 4D35-TG Silicon Graphics Workstation with a 60 Hz raster frequency. In all cases the stimuli were Gaussian blobs (σ = 0.65 deg) of either positive or negative polarity (Michelson contrast = 0.43) presented on a gray background of 31 cd/m^2 and subtending 8.4 × 6.8 deg at 57 cm from the observer. In all cases, the Gaussian blobs appeared on a circular trajectory around fixation (marked by a central black square) with a 5.25 deg radius.

The reference linear velocities of the drifting or flashed blobs were 1, 5 or 10 deg/s.

STV experiments (Fig. 2, top)

Two Gaussian blobs of opposite polarities appeared simultaneously 90 deg (of circle) apart at a random position on the virtual circle and drifted divergently at the same velocity (1, 5 or 10 deg/s) for a randomized duration (375 ± 125 ms). They disappeared simultaneously and only one of them (randomly chosen from trial to trial) reappeared after a variable duration Δt (33, 67, 133, 267 or 533 ms; the independent variable)

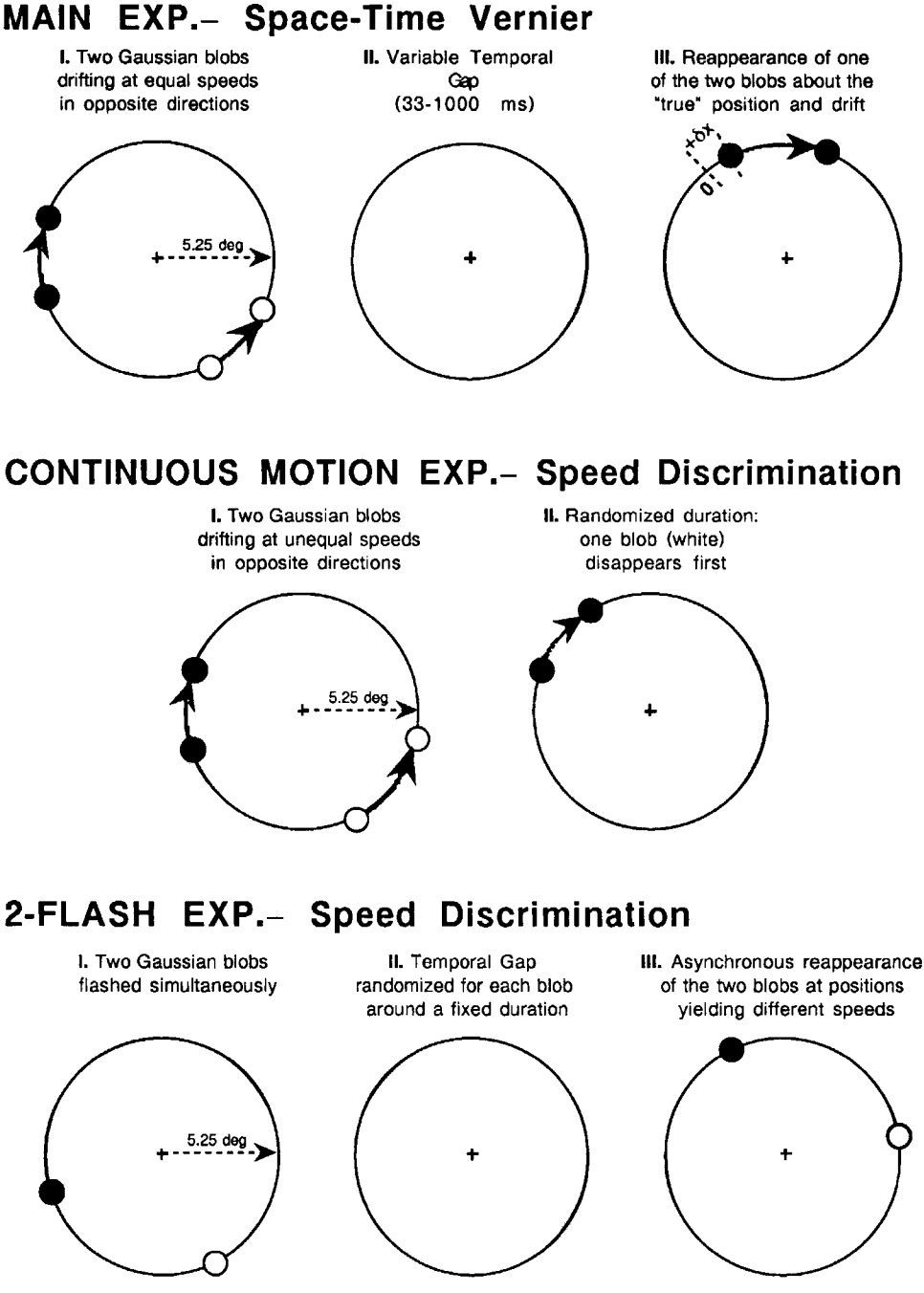

Figure 2. The three experimental configurations. Black and white disks stand for Gaussian blobs of opposite polarities. Blobs were constrained to drift or jump along a circular trajectory around fixation (large circles). See text for more details.

at a variable spatial offset, δx (dependent variable) relative to where it should have reappeared on the assumption of a constant V; the blob then continued to drift for a randomized duration (375 ± 125 ms). The observer had to decide whether δx was positive or negative with respect to the 'true' (0) position. The presence of the two blobs before their disappearance ensured that systematic eye pursuit was impossible (see Note 5).

Speed discrimination with continuous motion (*CM experiments*; Fig. 2, middle)

The two blobs appeared and drifted as in the STV experiment. One of the blobs always drifted at a 'reference' V (1, 5 or 10 deg/s), whereas the velocity of the second (dependent variable) was faster or slower. Their drift duration was randomized *independently* (375 ± 125 ms). The observer had to decide which of the two blobs drifted more rapidly.

'Velocity' discrimination with 2-Flashes stimuli (*2F experiments*; Fig. 2, bottom)

Two Gaussian blobs of opposite polarities were flashed simultaneously (for 66 or 133 ms) 90 deg (of circle) apart at a random position on the virtual circle, disappeared simultaneously and were flashed again after a duration ranging from $0.5\Delta t$ to $1.5\Delta t$ ms and randomized *independently* for each of them (with Δt, the independent variable). Δt could be 33, 67, 133, 267 or 533 ms. One of the blobs (whose polarity was randomly chosen) always reappeared at a position yielding the reference 'velocity' (1, 5 or 10 deg/s), whereas the second blob was spatially offset by $\pm\delta x$ (the dependent variable). The observer had to decide which of the two spatio-temporal jumps yielded the higher 'velocity'. The use of the quotation marks is meant to stress the fact that, with the exception of the two shortest durations, this 2F animation did not yield a real perception of motion. Given that the randomization of the duration of the temporal gap around Δt prevented the observer from basing his ('faster'/'slower') judgments on spatial or temporal cues alone, it must be concluded that, under conditions not yielding motion perception, such judgments required some sort of cognitive inference of V from independent estimations of temporal and spatial gaps.

In all three experiments the dependent variables (δx or V) were under the control of two interleaved modified PEST staircases (Taylor and Creelman, 1967) tracking the 25 and 75% correct ('faster' response) points which were computed as the mean of the last six of a total of ten reversals. In the STV and 2F experiments, one experimental session consisted in the assessment of the 25 and 75% points for each of the five Δt while the reference velocity was kept constant. The sequence of Δt was randomized across velocities, repeats (at least three but more frequently four) and observers and the sequence of velocities was randomized across repeats and observers. In the CM experiment, the 25 and 75% V-discrimination measurements were also randomized across repeats and observers. The three experiments were run separately in a different order for the two observers, the two authors, both emmetropic. The assessment of each pair (25 and 75%) of experimental points required ten-to-fifteen minutes (including preliminary sessions).

RESULTS

Figure 3 displays $-\delta x$ (circles) and $+\delta x$ (squares) thresholds (abscissa) as a function of Gap Duration (Δt) for all three experiments (CM: dotted and dashed lines; 2F: small, open symbols; STV: large solid symbols), for three velocities (different panels) and for observers AG (a) and SH (b). Thick, dashed lines in each panel are predictions of the STV thresholds based on the task 'decomposition' described above (see also Appendix). Thick continuous lines show the reference velocities. The main observations are as follows:

CM velocity discrimination (incremental and decremental) thresholds range between 40% (at 1 deg/s) and 31% (at 10 deg/s) for observer AG and in-between 28 and 17% for observer SH. They are substantially higher than those previously measured (e.g. McKee, 1981), but this difference may be due to at least three factors, namely the large size of the Gaussian blobs, their eccentric viewing and their circular trajectory. Also, CM incremental and decremental thresholds are fairly symmetric about the reference V along the x axis. When averaged across the three velocities and the two observers, they yield practically identical Weber fractions, i.e. $+27 \pm 4.3\%$ and $-28 \pm 4.6\%$, respectively. This equality of the positive and negative liminar *spatial* offsets yields an inequality of the liminar *temporal* offsets.

2F and STV incremental and decremental thresholds are by far higher than the CM thresholds (they may exceed 1000% see also Fig. 4) and, with a few exceptions, they increase monotonically with Δt. Also, they display strong asymmetries with respect to the reference V but the inferred points of subjective equality (PSE) do not yield any systematic pattern over experimental conditions or observers. Nonetheless, one can note a more or less systematic shift toward positive PSEs for the highest velocities (10 deg/s, for observer AG and 5 and 10 deg/s, for observer SH) and the largest Δt (267 and/or 533 ms). Such a positive PSE shift may be attributed to the fact that for these high velocities and long durations (and thus, long trajectories), the linear displacement subtended by the 2F motion and by the appearance and disappearance of the blobs in the STV condition yields significantly *slower* velocities than the circular trajectory for which their linear velocity was actually specified. It is also the case that in some conditions, what is perceived as being a velocity slower than the reference is in fact physically faster (all the circles which are on the right of the continuous thick line, the reference V).

2F thresholds are, in general, slightly higher than the STV ones (as they should be on the basis of the STV task decomposition described above). For the 1 deg/s condition and for both observers, all the decremental 2F thresholds (small, open circles) yield negative values the meaning of which is that, in order to be discriminated from a 1 deg/s velocity, slower velocities must also change sign, i.e. drift in the opposite direction. For the decremental STV thresholds, this is the case only for observer SH. Negative decremental thresholds are to be expected given that the velocity spectrum of short-duration moving and 2F stimuli does indeed include opposite sign velocities.

Returning to the hypothesis according to which STV can be reduced to a V-discrimination task (see the Introduction section), the STV (as well as the 2F) data show no significant deviation from linearity (as a function of Δt), i.e. they lie on

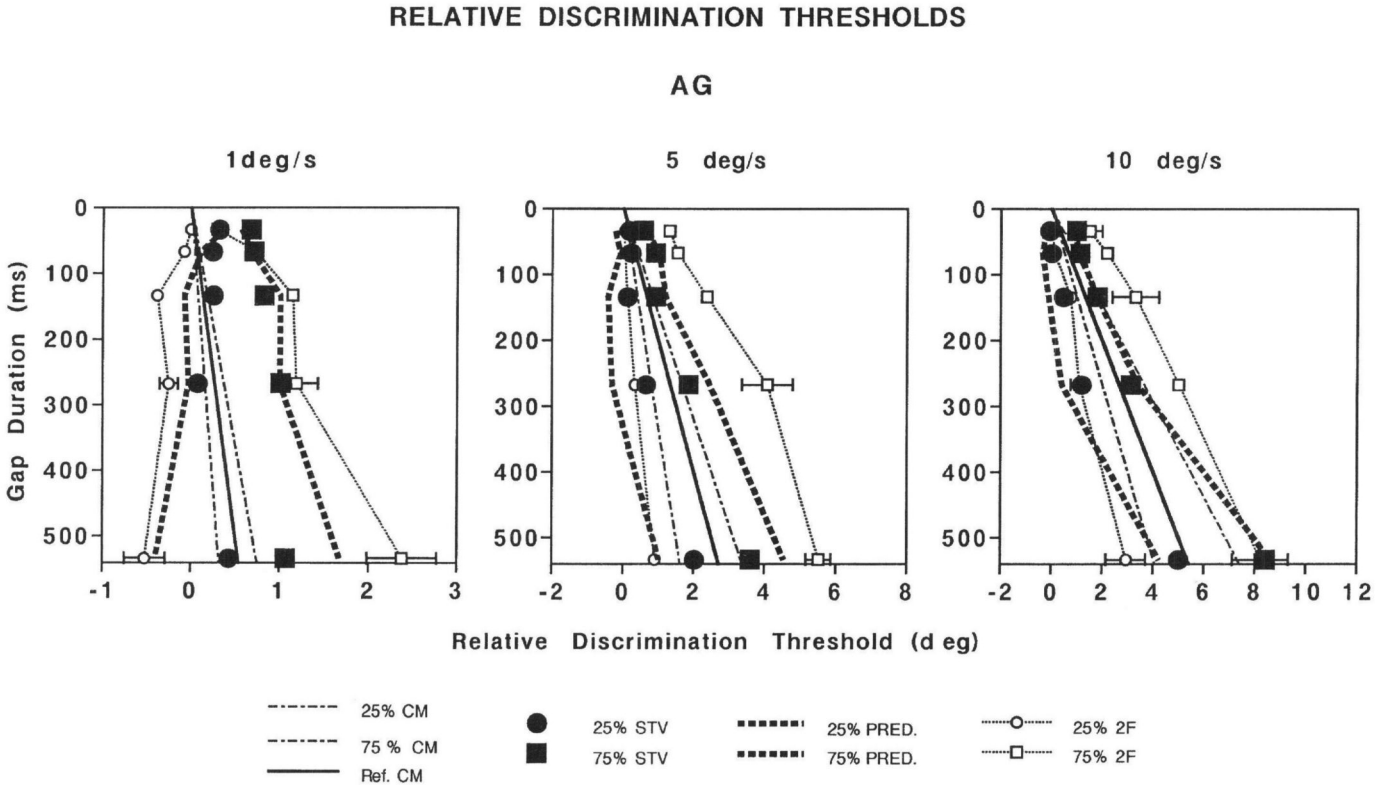

Figure 3. Discrimination thresholds for the three experiments (CM, 2F and STV) and STV predictions for observers AG (a) and SH (b). Different panels show data and predictions for different reference velocities. Small, open symbols and dotted lines are $-\delta x$ (circles) and $+\delta x$ (squares) thresholds (abscissa) measured as a function of Δt (ordinate) in the 2F experiment. Large, filled symbols are $-\delta x$ (circles) and $+\delta x$ (squares) thresholds measured in the STV experiment. Horizontal bars show ± 1 SE (when larger than the symbols). Straight, dashed and dotted lines are velocity discrimination thresholds from the CM experiment shown in the same $x-t$ space. Heavy dashed lines show predictions of the STV thresholds based on performances in the CM and 2F experiments.

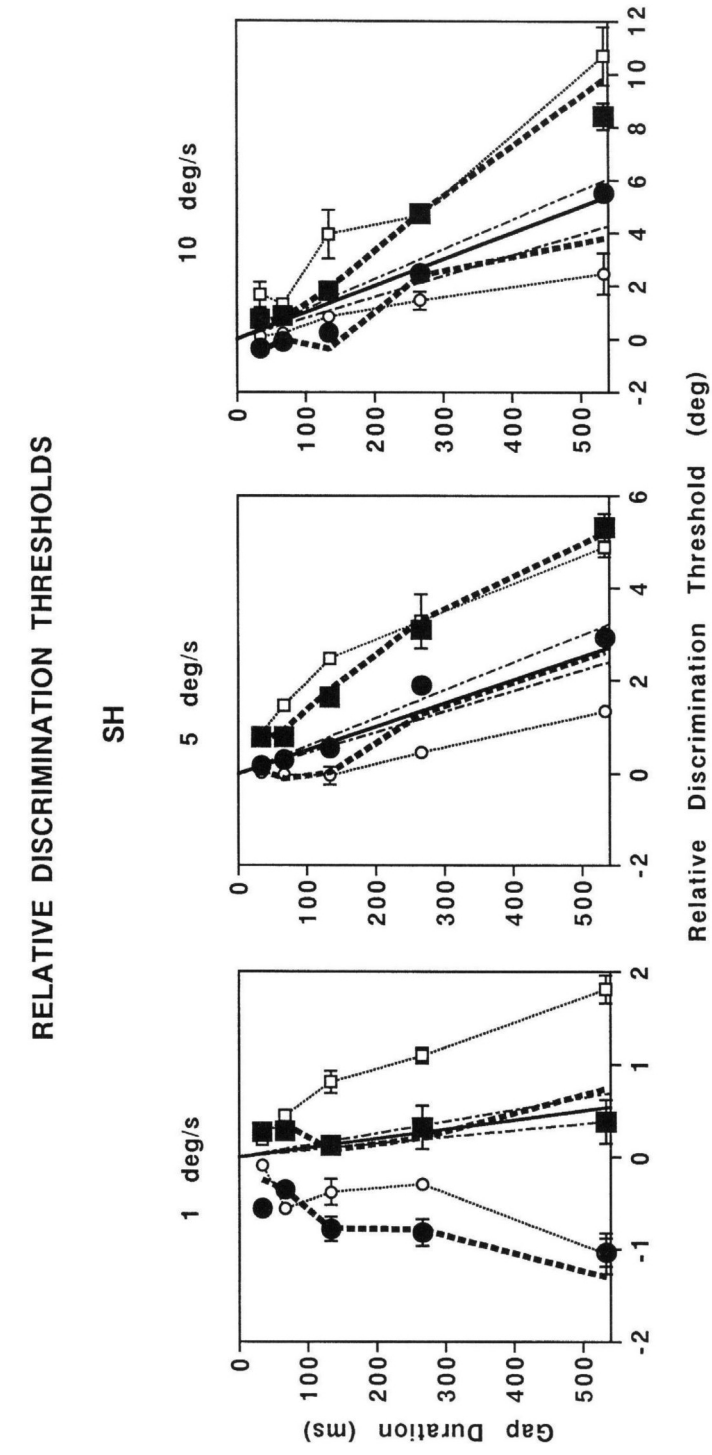

Figure 3. (Continued).

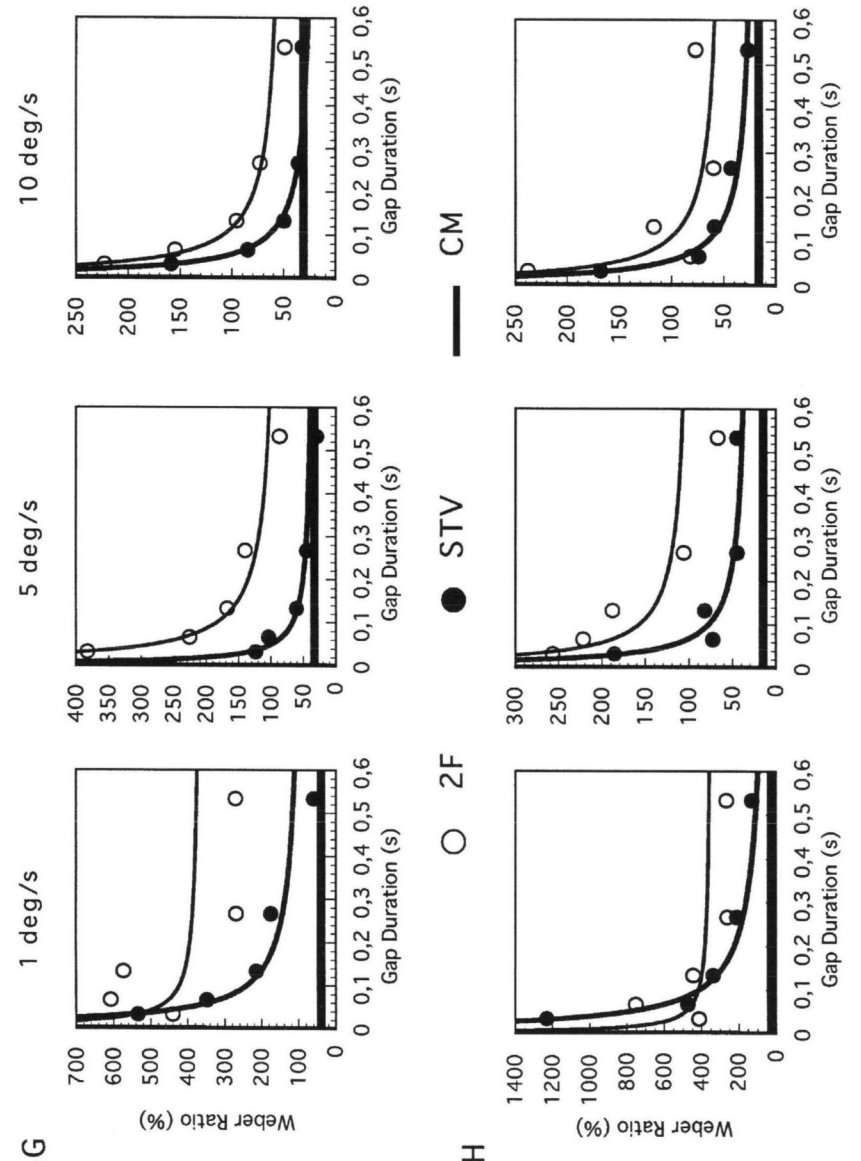

Figure 4. Mean discrimination thresholds expressed as Weber ratios ($WR = 100\delta x/\Delta x$ or, equivalently, $100\delta V/V$) as a function of gap duration (Δt) for 2F and STV experiments (open and filled circles, respectively). Weber ratios for the CM condition are shown as horizontal heavy lines. Continuous curves are fits of the data with the linear model described in the text. Upper and lower panels are for observers AG and SH.

a constant V line. This is the case at least for Δt as high as 267 ms beyond which the integration range of the underlying motion mechanisms is probably exceeded (see McKee and Welch, 1985). Within this range, a regression analysis did not reveal any significant nonlinear trends. All in all, the present data appear to support the V-discrimination hypothesis for the STV task.

Finally, the predictions of the STV data based on the task *decomposition* described in the Decomposition section above are reasonably accurate for Obs. SH and less so for Obs. AG, particularly for 1 and 5 deg/s conditions. All in all, however (and taking into account that the three experiments, CM, 2F and STV, were run in sequence over a period of about two months), these predictions support the proposed decomposition of the STV task.

The incremental and decremental thresholds displayed in Fig. 3 were averaged together (in absolute values) for each Δt, reference V and observer and are presented in Fig. 4 as Weber ratios ($WR = 100\delta x/\Delta x$ or, equivalently, $100\delta V/V$) as a function of Gap Duration (Δt) for 2F and STV experiments (open and solid circles, respectively). Weber ratios for the CM condition are shown as horizontal heavy lines.

The data are reasonably well fit by arbitrary power functions (not shown; $r^2 > 0.9$ with the exception of the 1 deg/s condition). In line with our V-discrimination hypothesis, a meaningful fit, however, could be based on the single postulate that δx thresholds lie on a straight line (i.e. a constant V) with a non-zero intercept which stands for the *minimum displacement* threshold, $d_{\min}$ (see Fig. 1b). δx is then given by:

$$\delta x = t(V - V_0) + d_{\min},$$

and the Weber ratio by:

$$WR(\Delta t) = K_1 + K_2/t,$$

where $K_1 = (V - V_0)/V_0$ and $K_2 = d_{\min}/V_0$, with V_0 the reference velocity. Fitting the model to the data amounts thus to finding the best fits of V and $d_{\min}$ (or, equivalently, $t_{\min} = -d_{\min}/V$). The $WR(\Delta t)$ fits are shown as continuous curves in Fig. 4. They yield r^2 coefficients at least as high as those obtained with the arbitrary power functions ($r^2 > 0.9$ with the exception of the 2F, 1 deg/s condition where they are below 0.2 for both observers). Thus, the present derivation of the theoretical $WR(\Delta t)$ functions provides additional support to our working hypothesis.

The main observation from both the measured and predicted Weber ratios is that they steeply decrease with Δt up to about 100–200 ms and reach an asymptotic regime thereafter. This behavior is to be expected given that the discriminable V does not pass through the origin of space–time (i.e. the dynamic $d_{\min}$ and $t_{\min}$ are non-zero). The steep decrease for small spatio-temporal gaps is equivalent to the 'crowding' effect described by Levi and Klein (1990) in a purely spatial task. For large Δt, the STV Weber ratios tend to approach those measured in the CM experiment. The 2F Weber ratios are systematically higher than the STV ones (as they should be given the decomposition of the STV task).

Figure 5 displays the estimated K_1 parameters (i.e. $(V - V_0)/V_0$; not to be confounded with the WRs of Fig. 4 which include $d_{\min}$) for the STV and 2F tasks and the $\delta V/V$ ratios actually measured in the CM task. As expected from the literature,

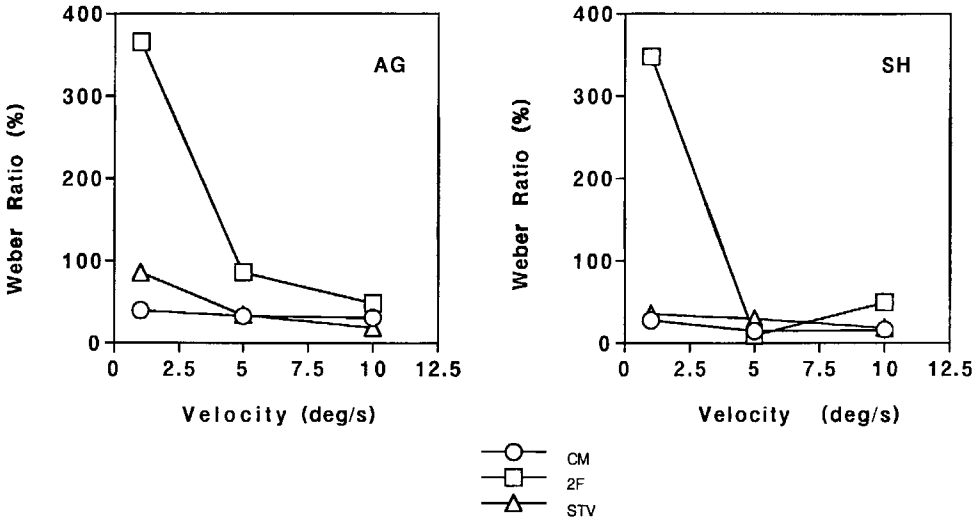

Figure 5. Weber ratios computed as a function of velocity for CM, 2F and STV experiments (circles, squares and triangles, respectively) and for observers AG (left) and SH (right). The computation is based on the estimated $x-t$ slopes of the 2F and STV δx vs Δt functions and ignores their intercepts at the origin. See text for more details.

the CM Weber ratios are practically independent of V in the inspected range although they are significantly larger than previously reported (see above). Note the close match between the CM performances (circles) and the estimated STV ones (triangles) the meaning of which is that CM and STV tasks yield practically identical $\delta V/V$ ratios. This observation reinforces the notion that STV is a velocity discrimination task. The $\delta V/V$ ratios estimated from the 2F experiment are appreciably higher only for the slower velocity (1 deg/s) probably because of the widely spread spatio-temporal spectrum of these animations.

The spatial ($d_{\min}$) and temporal ($t_{\min}$) offsets at the origin of space-time derived from the fitting procedure described above are displayed in Fig. 6a and b, respectively. Whilst we are not aware of any estimation of $t_{\min}$ (as defined here; see Fig. 1b) in the literature, $d_{\min}$ estimates have been previously obtained only from two-flash experiments which do not allow their assessment as a function of velocity (see Baker and Braddick, 1985a, b). In the present work, $d_{\min}$ and $t_{\min}$ are *dynamic* in the sense that they are estimated for drifting targets (see their definition in the section on the Analysis of the STV task).

Intuitively, the higher the reference velocity, the larger the instantaneous spatial jump (i.e. dynamic $d_{\min}$) and the shorter the motion stop (dynamic $t_{\min}$) required to make such a perturbed drift discriminable from a continuous one. For the 2F experiment, the dynamic $d_{\min}$ follows indeed this trend: it ranges for both observers from about 0.065 deg at 1 deg/s to about 0.6 deg at 10 deg/s. For the STV experiment, $d_{\min}$ is more or less constant for both observers up to at least 5 deg/s (about 0.16 and 0.31 deg for AG and SH, respectively) and increases to about 0.47 deg at 10 deg/s. All in all, the general tendency is an increase of the dynamic $d_{\min}$ with V.

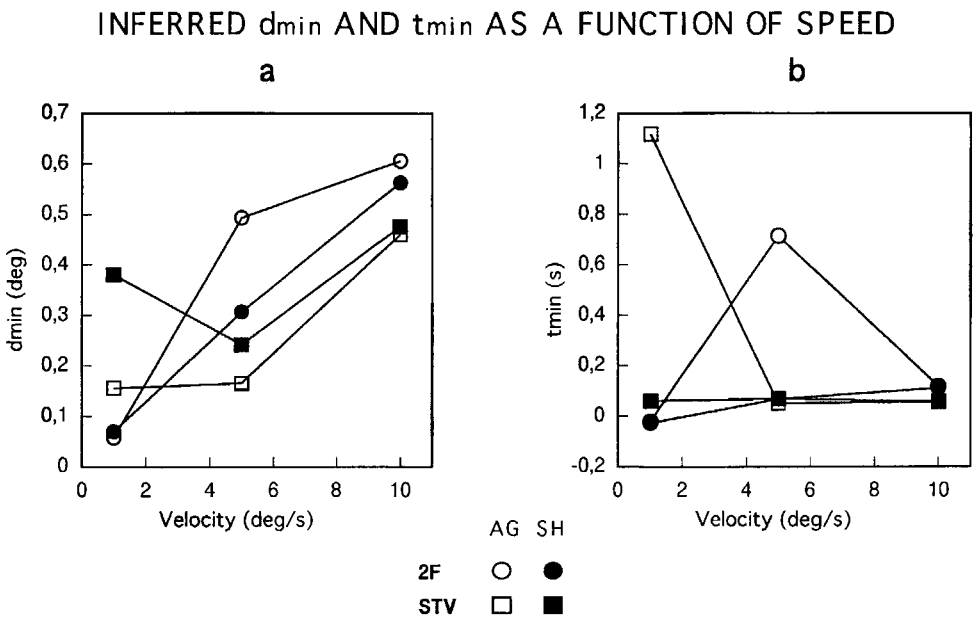

Figure 6. Inferred *dynamic* d_{min} (a) and t_{min} (b) offsets as a function of velocity for observers AG (open symbols) and SH (filled symbols) and for 2F (circles) and STV (squares) tasks.

With one exception (Obs. AG at the slowest tested V for the STV experiment), the inferred dynamic t_{min} is more or less independent of V and equal, in average, to 50–60 ms.[6] This contrasts with the intuitive prediction of a decreasing t_{min} with V.

DISCUSSION

To our knowledge, this work presents the first *direct* assessment of the spatio-temporal vernier acuity and of velocity discrimination with 2F stimuli. STV was analyzed from two independent perspectives both of which pose that STV *is reducible to a velocity discrimination task*. The 'empirical' approach consisted in decomposing the task into a sequence of three velocity judgments the third of which (STV) is derived from the preceding two (CM and 2F). Given their variability, this empirical model provides reasonable fits to the STV data. The theoretical approach capitalized on the notion that STV performances reflect the velocity discrimination capacities of the visual system. Accordingly, it predicted that STV performances as a function of Δt should lie on a straight line in space-time (i.e. a constant V) with a non-zero intercept at the origin of space-time and that the slope of this line should coincide with the minimum discriminable V in a standard CM experiment. The measured STV functions (i.e. $\pm\delta x$ as a function of Δt) are consistent with both these predictions strongly suggesting that the STV task is indeed equivalent to a V-discrimination task. Whilst the linearity prediction might have been inferred from the observation that spatial and temporal offsets of moving targets appear to compensate linearly (Morgan, 1976, 1979, 1980; Burr, 1979; Fahle and Poggio, 1981), the equivalence between the slope of the STV

thresholds (with Δt) and the $\Delta V/V$ ratio assessed in the CM experiment is not derivable from previous studies.

The present work introduced the notion of *dynamic* $d_{\min}$ and $t_{\min}$ and estimated their values from both 2F and STV experiments. These two quantities may be related (although not necessarily in a trivial way) to the spatial and temporal impulse responses of the underlying motion sensors. Accordingly, the observed increase of the dynamic $d_{\min}$ with V reflects the correlative decrease in the spatial frequency characteristic of the optimal subserving motion units (see Chung *et al.*, 1996). The $d_{\min}$ estimates for the 2F task (see Fig. 6, circles) range from about 0.065 deg (for 1 deg/s) to about 0.6 deg (for 10 deg/s). On the assumption of a direct proportionality between these spatial constants and the peak spatial frequency characteristic of the motion sensors, the latter should range from about 15 to 1.7 c/deg, respectively. For the STV task, the estimated $d_{\min}$ (Fig. 6, squares) is about constant up to 5 deg/s (0.23 deg) and increases to about 0.47 deg at 10 deg/s. This yields a peak frequency range from 4.3 to 2.1 c/deg.[7] Whilst the specific relationship between dynamic $d_{\min}$ and peak spatial frequency requires further theoretical analysis, the view that higher velocities are processed by lower spatial frequency units is entertained in the literature at least since Kelly's (1979) work.

The estimated dynamic $t_{\min}$ is, with one exception (see Fig. 6), more or less independent of V. The average $t_{\min}$ is about 55 ms, close to the temporal integration limit inferred from temporal summation experiments (Gorea and Tyler, 1986). Current modeling of, as an example, motion blur (Pääkkönen and Morgan, 1994), also assumes a constant temporal integration characteristic with V. Experimental estimates of this variable show only small (less than a factor of two) variations with either spatial frequency (Gorea and Tyler, 1986), or velocity (Burr *et al.*, 1986). Different experimental approaches may yield larger variations (Hess and Snowden, 1992) but, in general, they are all within less than 200 ms (50 ms, according to Gorea and Tyler, 1986). To reach that level of temporal resolution, $t_{\min}$ should be measured directly (not estimated as it was here) on higher temporal resolution displays. Alternatively, once the linearity between δx and Δt is established, repeated $\pm\delta x$ measurements for only two temporal gaps should provide more accurate estimates of the spatial and temporal intercepts. In all events, the present estimates of $d_{\min}$ and $t_{\min}$ are in support of space-time separability at least within the tested velocity range.

When discussing STV functions, the question arises as to whether, and for what reason, they should be symmetrical with respect to the reference velocity. In fact, the same question could have been raised in relation to standard incremental and decremental velocity discrimination performances. As noted in the Introduction, all the previous studies we know of assumed these thresholds to be equal (i.e. equal incremental and decremental Weber ratios for velocity discrimination; e.g. McKee, 1981; McKee *et al.*, 1986; De Bruyn and Orban, 1988). Whilst the $\pm\delta x$ thresholds measured in the 2F and STV experiments display large and unsystematic asymmetries, the incremental and decremental velocity discrimination ratios measured in the CM experiment are practically equal thereby confirming the usual assumption. Equal incremental and decremental V-discrimination ratios guarantee that, in a space–time plot, the reference velocity V is *not* the bisector of the spatio-temporal angle formed

by the two discriminable velocities. Specifically, the reference V is tilted away from the bisector and toward the t-axis by an angle dependent on V. This asymmetry must relate one way or another to the asymmetric structure of space-time in motion perception (e.g. Burt, 1987). This observation sets a limit to the analogy between space-space and space-time orientation.

Acknowledgements

Supported by a grant 95-1195/A000/DRET/DS/DR to A. Gorea and by a Wellcome European Research Fellowship to S. T. Hammett. The material described in this paper was originally presented under the same title and the same authorship in ARVO, 1996 (*Invest. Ophtal. Vis. Sci.* **37** (Suppl.), S735).

NOTES

1. The literature strongly suggests that acceleration detection is based on V-discrimination rather than on acceleration-dedicated detectors (Werkhoven *et al.*, 1992; Snippe and Werkhoven, 1993; Simpson, 1994).

2. For example, Wilson's line element model predictions of two line separation discrimination (see Fig. 12.4 in Wilson, 1991) displays Weber's law behavior within a separation range well below the one observed in empirical studies. Moreover, the predicted thresholds show characteristic notches produced by transitions across different filter sizes which are not observed in the empirical data.

3. That is to say that the *slope* of the function relating vernier thresholds to separation be identical with the orientation (or velocity) just discriminable from a reference.

4. The literature typically provides V-discrimination thresholds as the absolute mean of the measured incremental and decremental thresholds (e.g. McKee, 1981; McKee *et al.*, 1986; De Bruyn and Orban, 1988). The underlying assumption is that the incremental and decremental Weber's fractions are equal, the consequence of which is that the reference V *cannot* be the bisector of the two discriminable speeds (see also the Discussion section).

5. On the assumption of an involuntary eye pursuit of the *critical* target, the resolution of the STV task could be based on a comparison between the position of re-appearance of this target and the position of the eye, given that *pursuit inertia* is observed for at least 300 ms (Mitrani and Dimitrov, 1978). As it is explained in the Methods section, this strategy was not workable in the present experiments: the simultaneous appearance of *two* targets drifting *divergently* precluded the possibility of knowing which of the two was the *critical* one.

6. It should be remembered that $d_{\min}$ and $t_{\min}$ were estimated through a fitting procedure where $d_{\min}$ and V (the discriminable velocity) were free parameters allowing for $t_{\min}$ $(= -d_{\min}/V)$ to covary with $d_{\min}$ and with $1/V$ (see Baker and Braddick, 1985b).

7. These particular peak spatial frequency ranges should depend on the σ of our Gaussian blobs; smaller $d_{\min}$ should be expected for smaller σ (see McKee, 1991, p. 230).

REFERENCES

Adelson, E. H. and Bergen, J. R. (1985). Spatiotemporal energy models for the perception of motion. *J. Opt. Soc. Am. A* **2**, 284–299.

Adelson, E. H. and Bergen, J. R. (1991). The plenoptic function and the elements of early vision. In: *Computational Models of Visual Processing*. M. S. Landy and J. A. Movshon (Eds). MIT Press, Cambridge, MA, pp. 1–20.

Andrews, D. P., Butcher, A. K. and Buckley, B. R. (1973). Acuities for spatial arrangement in line figures: Human and ideal observers compared. *Vision Res.* **13**, 599–620.

Baker, C. L. and Braddick, O. J. (1985a). Eccentricity-dependent scaling of the limits for short-range apparent motion perception. *Vision Res.* **25**, 803–812.

Baker, C. L. and Braddick, O. J. (1985b). Temporal properties of the short-range process in apparent motion. *Perception* **14**, 181–192.

Burbeck, C. A. (1987). Position and spatial frequency in large-scale localization judgments. *Vision Res.* **27**, 417–427.

Burbeck, C. A. (1988). Large-scale localization across spatial frequency channels. *Vision Res.* **28**, 857–859.

Burbeck, C. A. and Yap, Y. L. (1990). Two-mechanisms for localization? Evidence for separation-dependent and separation-independent processing of position information. *Vision Res.* **30**, 739–750.

Burr, D. C. (1979). Acuity for apparent vernier offset. *Vision Res.* **19**, 835–837.

Burr D. C, Ross, J. and Morrone, M. C. (1986). Seeing objects in motion. *Proc. R. Soc. London B* **227**, 249–265.

Burt, P. J. (1987). The interdependence of temporal and spatial information in early vision. In: *Vision, Brain, and Cooperative Computation*. M. A. Arbib and A. R. Hanson (Eds). MIT Press, Cambridge, MA, pp. 264–277.

Carney, T. and Klein, S. A. (1997). Resolution acuity is better than vernier acuity. *Vision Res.* **37**, 525–539.

Chung, S. T. L., Levi, D. M. and Bedell, H. E. (1996). Ricco's diameter for line detection increases with stimulus velocity. *J. Opt. Soc. Am. A* **13**, 2129–2134.

De Bruyn, B. and Orban, G. A. (1988). Human velocity and direction discrimination measured with random dot patterns. *Vision Res.* **28**, 1323–1335.

Fahle, M. and Poggio, T. (1981). Visual hyperacuity: spatiotemporal interpolation in human vision. *Proc. R. Soc. London B* **213**, 451–477.

Gorea, A. and Tyler, C. W. (1986). New look at Bloch's law for contrast. *J. Opt. Soc. Am. A* **3**, 52–61.

Hess, R. F. and Snowden, R. J. (1992). Temporal properties of human visual filters: number, shapes and spatial covariation. *Vision Res.* **32**, 47–59.

Hu, Q., Klein, S. A. and Carney, T. (1993). Can sinusoidal vernier acuity be predicted by contrast discrimination? *Vision Res.* **33**, 1241–1258.

Kelly, D. H. (1979). Motion and vision. II. Stabilized spatio-temporal threshold surface. *J. Opt. Soc. Am.* **69**, 1340–1349.

Klein, S. A., Casson, E. and Carney, T. (1990). Vernier acuity as line and dipole detection. *Vision Res.* **30**, 1703–1719.

Levi, D. M., Klein, S. A. and Yap, Y. L. (1988). 'Weber's law' for position: Unconfounding the role of separation and eccentricity. *Vision Res.* **28**, 597–603.

Levi, D. M. and Klein, S. A. (1990). The role of separation and eccentricity in encoding position. *Vision Res.* **30**, 557–585.

Macmillan, N. A. and Creelman, C. D. (1991). In: *Detection Theory: A User's Guide*. Cambridge Univ. Press, Cambridge, pp. 67–70.

McKee, S. P. (1981). A local mechanisms for differential velocity detection. *Vision Res.* **21**, 491–500.

McKee, S. P. (1991). The physical constraints on visual hyperacuity. In: *Limits of Vision*. J. J. Kulikowski, V. Walsh and I. J. Murray (Eds). CRC Press, Boca Raton, pp. 221–233.

McKee, S. P., Silverman, G. H. and Nakayama, K. (1986). Precise velocity discrimination despite random variations in temporal frequency and contrast. *Vision Res.* **26**, 609–619.

McKee, S. P. and Welch, L. (1985). Sequential recruitment in the discrimination of velocity. *J. Opt. Soc. Am. A* **2**, 243–251.

Mitrani, L. and Dimitrov, G. (1978). Pursuit eye movements of a disappearing moving target. *Vision Res.* **18**, 537–539.
Morgan, M. J. (1976). Pulfrich effect and the filling in of apparent motion. *Perception* **5**, 187–195.
Morgan, M. J. (1979). Perception of continuity in stroboscopic motion: a temporal frequency analysis. *Vision Res.* **19**, 491–500.
Morgan, M. J. (1980). Spatiotemporal filtering and the interpolation effect in apparent motion. *Perception* **9**, 161–174.
Morgan, M. J. (1991). Hyperacuity. In: *Vision and Visual Dysfunction, Vol. 10, Spatial Vision*. D. Regan (Ed.). CRC Press, Boca Raton, pp. 87–113.
Morgan, M. J. and Aiba, T. S. (1985). Vernier acuity predicted from changes in the light distribution of the retinal image. *Spatial Vision* **1**, 151–161.
Morgan, M. J., Hole, G. J. and Ward, R. M. (1990). Evidence for positional encoding in hyperacuity. *J. Opt. Soc. Am. A* **7**, 297–304.
Pääkkönen, A. K. and Morgan, M. J. (1994). Effects of motion on blur discrimination. *J. Opt. Soc. Am. A* **11**, 992–1002.
Simpson, W. A. (1994). Temporal summation of visual motion. *Vision Res.* **34**, 2547–2559.
Snippe, H. P. and Werkhoven, P. (1993). Pulse modulation in human motion vision. *Vision Res.* **33**, 647–656.
Taylor, M. M. and Creelman, C. D. (1967). PEST: Efficient estimates on probability functions. *J. Opt. Soc. Am.* **41**, 782–787.
Watt, R. J. (1987). Scanning from coarse to fine spatial scales in the human visual system after the onset of the stimulus. *J. Opt. Soc. Am. A* **4**, 2006–2021.
Watt, R. J. and Morgan, M. J. (1983). Mechanisms responsible for the assessment of visual location: theory and evidence. *Vision Res.* **23**, 97–109.
Watt, R. J., Morgan, M. J. and Ward, R. M. (1983). The use of different cues in vernier acuity. *Vision Res.* **23**, 991–995.
Werkhoven, P. and Koenderink, J. J. (1991). Visual processing of rotary motion. *Perception and Psychophys.* **49**, 73–82.
Werkhoven, P., Snippe, H. P. and Toet, A. (1992). Visual processing of optic acceleration. *Vision Res.* **32**, 2313–2329.
Wilson, H. R. (1985). Discrimination of contour curvature: data and theory. *J. Opt. Soc. Am. A* **2**, 1191–1199.
Wilson, H. R. (1986). Responses of spatial mechanisms can explain hyperacuity. *Vision Res.* **26**, 453–469.
Wilson, H. R. (1991). Pattern discrimination, visual filters, and spatial sampling irregularity. In: *Computational Models of Visual Processing*. M. S. Landy and J. A. Movshon (Eds). MIT Press, Cambridge, MA, pp. 153–168.
Wilson, H. R. and Gelb, D. J. (1984). Modified line element theory for spatial frequency and width discrimination. *J. Opt. Soc. Am. A* **1**, 124–131.

APPENDIX: PREDICTING STV FROM CM AND 2F SPEED DISCRIMINATION THRESHOLDS

d', the sensitivity in the CM task is given by

$$d'_{\mathrm{CM}} = \frac{\Delta x_{\mathrm{CM}}}{s_{\mathrm{CM}}}, \tag{A1.1}$$

with s_{CM}, the standard deviation of the noise in this task normalized to 1; equivalently

$$d'_{\mathrm{2F}} = \frac{\Delta x_{\mathrm{2F}}}{s_{\mathrm{2F}}}. \tag{A1.2}$$

Given that we worked at a constant performance level,

$$d'_{CM} = d'_{2F} \Rightarrow s_{2F} = \frac{\Delta x_{2F}}{\Delta x_{CM}}. \tag{A1.3}$$

The STV task being modeled as the comparison between the estimated velocities in CM and 2F conditions — each estimation yielding a different variance — and given standard d' recipes (see (Macmillan and Creelman, 1991), it follows from equations (A1.1)–(A1.3):

$$d'_{STV} = \frac{\Delta x_{STV}}{\sqrt{\dfrac{1 + \left(\dfrac{\Delta x_{2F}}{\Delta x_{CM}}\right)^2}{2}}}. \tag{A1.4}$$

Because

$$d'_{CM} = d'_{2F} = d'_{STV} \Rightarrow d'_{STV} = \Delta x_{CM}, \tag{A1.5}$$

it follows from equations (A1.4)–(A1.5) that Δx_{STV} (the sought-after variable) is given by:

$$\Delta x_{STV} = \Delta x_{CM} \sqrt{\frac{1 + \left(\dfrac{\Delta x_{2F}}{\Delta x_{CM}}\right)^2}{2}}. \tag{A1.6}$$

Measured PSE offsets were subtracted from the values of Δx_{CM} and Δx_{2F} and were added to the predicted Δx_{STV}.